

● Multimodal Chemical Imaging to probe Alzheimer's Disease Pathology

MALDI Imaging has emerged as a valuable tool for understanding neurodegenerative pathology in Alzheimer's disease.

Abstract

Already affecting 12% of population over the age of 65, and with an exponential increase in prevalence, Alzheimer's disease presents a global health challenge. There is no cure since the chain of molecular events underlying

disease pathogenesis remain unclear. Amyloid plaque formation, and tau protein aggregation constitute the major pathological hallmark and have been long considered to be central in pathogenesis. Common tools used in biochemical research lack broadband specificity and

sensitivity to study disease progression at the molecular level. However, alternative chemical imaging approaches based on MALDI Imaging mass spectrometry are proving to be quite valuable, as demonstrated here.

Keywords:
MALDI Imaging,
Alzheimer's disease,
amyloid plaque
pathology

Introduction

The prevalence of age associated diseases such as neurodegenerative disorders including Alzheimer's disease is increasing dramatically as the average age of the world's population increases.

Alzheimer's disease (AD) poses an immense societal challenge, particularly as there are still no curative treatments as the pathogenic mechanisms of AD remain elusive. The major hallmark of AD is the progressive accumulation of beta amyloid peptides derived from amyloid

precursor protein (APP) and hyper-phosphorylated-Tau protein, into extra- and intra-cellular deposits [1].

The prominent role of amyloid plaque pathology has long been recognized in AD. Overall molecular processes underlying mechanisms that lead

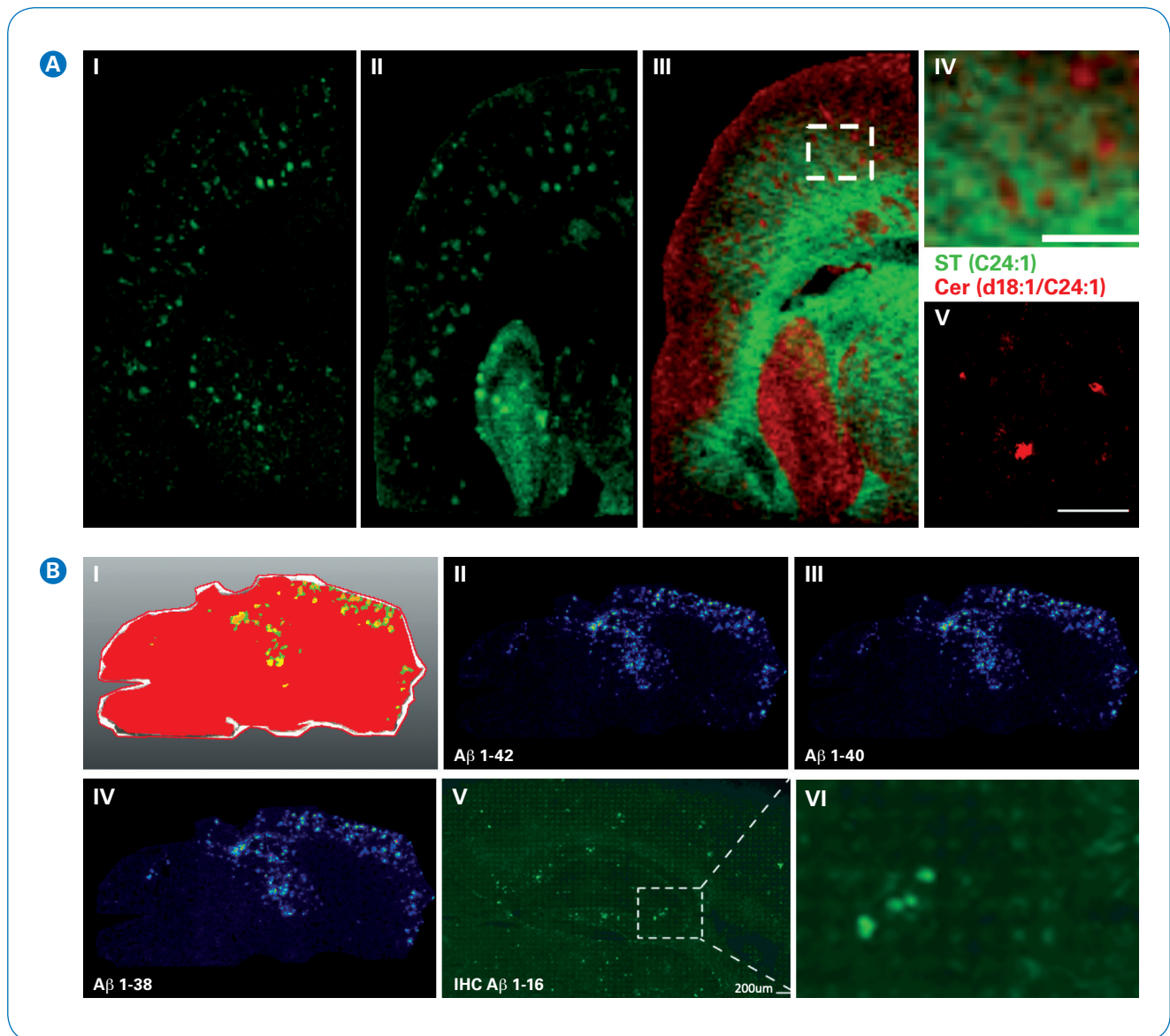


Figure 1: Previous work on using MALDI Imaging for probing amyloid plaque pathology associated lipids (A) (I-V) and Aβ peptides (B) (I-VI) in 18-month old transgenic Alzheimer's disease model mice (tgAPPArcSwe). (A) MALDI based lipid imaging of tgAPPArcSwe mouse brain tissue revealed increased sphingolipids (gangliosides and ceramides) including gangliosides (eg. GM3 d18:1/C:18; m/z 1383) (A) (I) and ceramides (e.g. Cer d18:1/24:1, m/z 646.5) (A) (III). In contrast sulfatides, such as sulfatide ST (24:1), m/z 888.6; were found to be significantly decreased in the deposits as further illustrated by the overlay of ST (C24:1), (Green); and Cer (d18:1/C24:1), (Red), which is representing the corresponding ceramide base. (A) (III) Magnification of highlighted insert (A) (IV) in the lateral Ctx. A-V) Complementary immunohistochemistry validates Aβ identity (Scale bars IV, V: 200um). (B) (I) Image analysis using hierarchical cluster analysis (HCA, bisecting k-means) delineates histological features resembling plaque pathology (yellow and green features). (B) (II-IV), Inspection of the corresponding variables in the clusters that cause this difference, reveals major Aβ species. (B) (V-VI) The IMS staining experiments were complemented with immunohistochemistry (IHC) towards Aβ on the same section to verify the Aβ identity of these plaques in general (B) (V); scale 1mm; A-VI: 200um).

to both neurodegenerative A β and Tau pathology in AD are not well characterized, particularly, since some cognitively normal patients also present with age-associated extracellular A β plaques and are hence referred to as cognitively- unaffected amyloid-positive (CU-AP)

[2]. An exact understanding of amyloid pathology is further complicated by presentation of heterogeneous amyloid aggregates that precipitate as structurally distinct plaque morphotypes such as diffuse and cored plaques. Distinct clouds of amyloid polymorphism have further

been associated with heterogeneous AD pathology and autosomal dominant mutations in familial AD.

A major challenge in investigating A β pathology and amyloid polymorphism is the need for appropriate imaging technologies that provide the

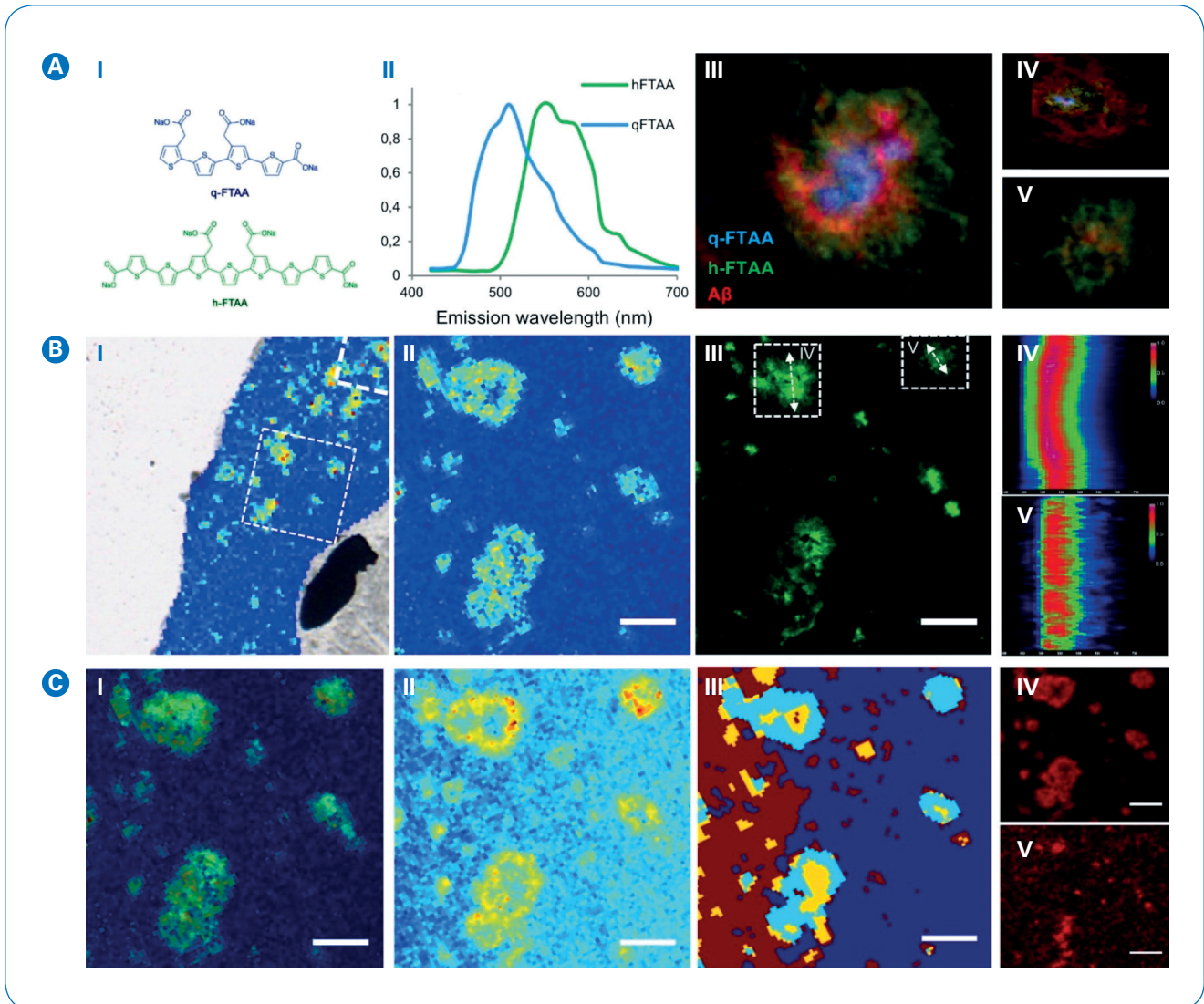


Figure 2: Multimodal chemical imaging to probe amyloid pathology in situ. (A) Amyloid polymorphism can be delineated with luminescent conjugated oligothiophene (LCO) probes including (quattro- (q-) and heptameric (h-) formyl-thiopheneacetate (FTAA)). These probes stain different amyloid aggregates and are used to delineate plaque polymorphism. (A) (III) LCO probes have different absorption and emission properties, which facilitates multiplexed staining and hyperspectral fluorescent imaging. (A) (III) Here, q-FTAA stains preferably compact fibril structures (core: blue (A) (III), (A) (IV) in A β pos. plaques (red), while h-FTAA stains more diffuse assemblies (green) i.e. corona in cored plaques (A) (III) or diffuse plaques (A) (V). (B) Multimodal imaging using IMS (B) (II) and LCO staining (B) (III) on the same tissue in transgenic AD mice (tgSwe). Multimodal chemical imaging delineates peptide and lipid species associated with plaque polymorphism i.e. compact mature plaques (B) (IV) and diffuse deposits (B) (V) as revealed by their hyperspectral profile indicating a spectral shift over the core in mature plaques (B) (IV). (C) Image alignment (C) (I) followed by PCA (C) (II) and cluster analysis (C) (III) revealed peptide and lipid species associated with diffuse aggregates (ganglioside GM1, (C) (IV)) or with the core region of mature plaques (ceramide-1-phosphate, (C) (V)). Scalebar=30 μ m.

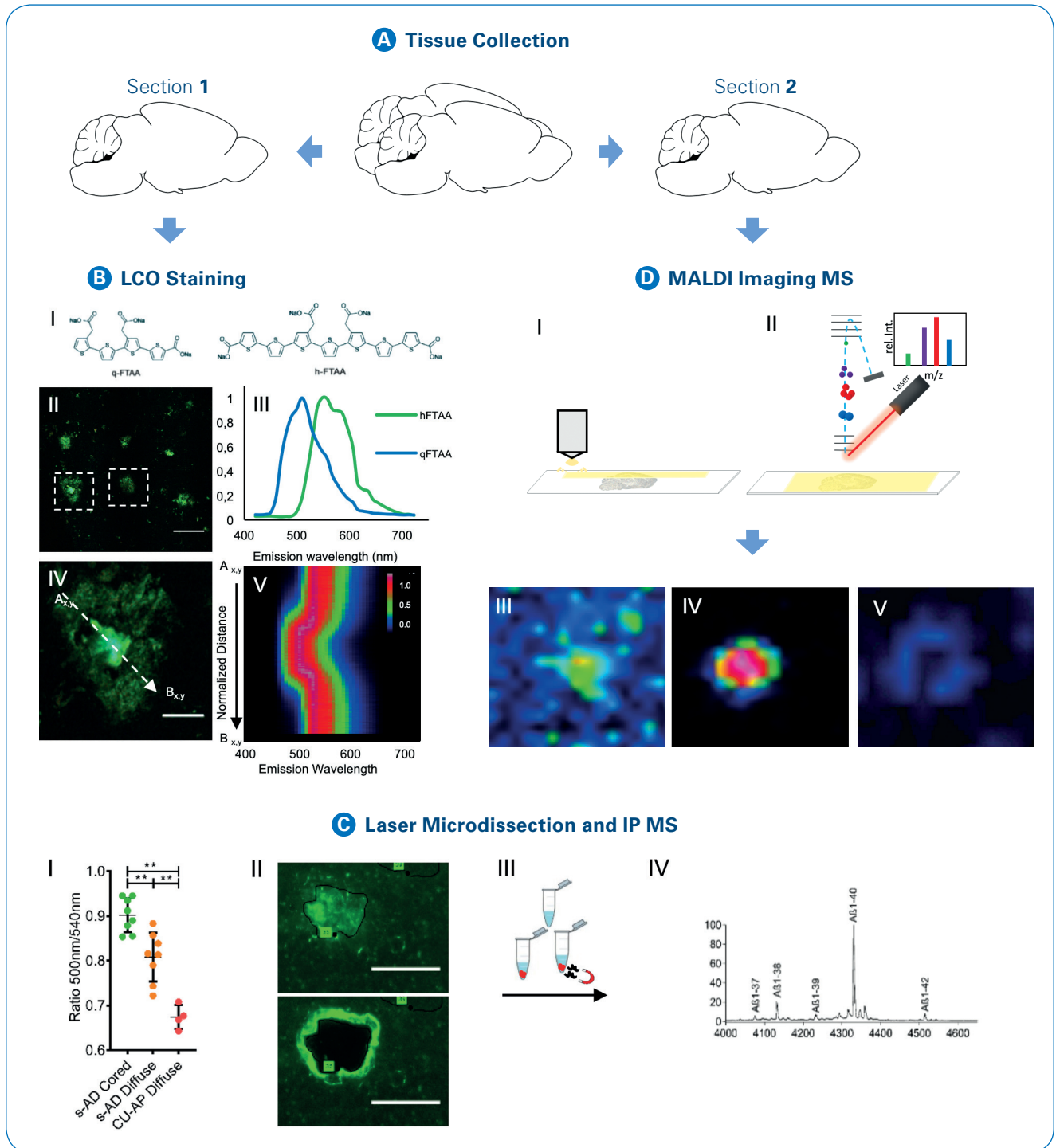


Figure 3: Experimental Setup. Multimodal chemical imaging paradigm for analysis of tgAPPSWE and s-AD/CU-AP brain tissue. **(A)** Cryo-sectioning and collection of 12 μm brains sections that were thaw-mounted onto LMD membrane slides for laser microdissection (Section 1) and onto conductive, indium tin oxide coated glass slides for MALDI Imaging mass spectrometry (Section 2). **(B)** (I) Section 1 was used for double staining with q- and h-FTAA. **(B)** (II) Fluorescence imaging of LCO stained plaque pathology followed by **(B)** (III) LCO spectral acquisition and **(B)** (IV,V) line scan analysis across polymorphic plaques. Here, **(B)** (IV) a blue shift indicates q-FTAA binding as observed for the core region of neuritic plaques in s-AD. **(C)** (I) Plaques morphotypes could be classified based on their hyperspectral profile and gave characteristic emission ratio values (500 nm/540 nm) corresponding to the degree of q- and h-FTAA content. **(C)** (II) Hyperspectrally delineated plaques were excised by laser microdissection. **(C)** (III) Plaques were extracted with formic acid followed by A β enrichment with Immunoprecipitation IP. **(C)** (IV) Individual A β species were identified and relatively quantified with MALDI mass spectrometry (see also Figure 1 **(B)**-**(D)**). **(D)** MALDI IMS was performed on consecutive sections (Section 2) to the sections used for LCO imaging and LMPC. Here, **(D)** (I) the tissue section was coated with crystalline, small organic matrix. **(D)** (II) This was followed by laser irradiation based desorption and ionization (MALDI) and ion detection with a time of flight mass analyzer generating MALDI TOF MS data from distinct coordinates of the tissue section. Acquisition of MALDI MS in a pre-defined pattern can generate distinct ion distribution map (single ion images). This is exemplified for A β peptides in human s-AD tissue with A β 1-42 localizing to diffuse plaques **(D)** (III) and A β 1-40 localizing to the center of cored plaques **(D)** (IV) as well as to CAA **(D)** (V).

necessary spatial resolution, sensitivity and molecular specificity. Over the last two decades MALDI Imaging has become a valuable technology of biomedical research and pathology. Our group has established a range of chemical imaging modalities, including MALDI Imaging, to probe chemical aspects of amyloid pathology in situ [3, 4, 5], and imaging of plaque-associated proteins and lipids with an emphasis on interfacing these analyses with subsequent immunohistochemistry and fluorescent microscopy [6] (Figure 1).

Most recently, we expanded this multimodal imaging toolbox to include structure-sensitive fluorescent amyloid probes [7]. Luminescent Conjugated Oligothiophenes (LCO) have different binding affinities towards different mature amyloid structures. Moreover, these probes have different electrooptical properties and thus different emission spectra that allow double staining and spatial delineation of differential LCO binding using fluorescent microscopy with spectrophotometry detection.

Results and Discussion

We employed our multimodal imaging strategy to gain a deeper understanding of biochemical distributions associated with plaque polymorphism. In detail, the LCO hyperspectral microscopy paradigm was interfaced with immunofluorescent staining as well as *in situ* MALDI Imaging and profiling to analyze both plaque associated lipids [8] and peptides [9]. An example of the strategy output is shown in Figure 2. Here, comprehensive imaging of amyloid polymorphism in transgenic mice identified different lipid species associated with plaque pathology.

More specifically, hyperspectral LCO and MALDI Imaging derived lipid signatures were acquired from the same tissue section. Comprehensive multivariate image analysis revealed ceramides and short-chain gangliosides localize to diffuse amyloid structures. In turn, ceramide-phosphate displayed a distinct correlation with cored, mature plaque structures indicating a role for these lipids in plaque maturation and formation of senile, neurotoxic deposits.

Most importantly, we were also able to characterize the actual A β peptides associated with plaque polymorphism. Attempts to combine fluorescent imaging and protein/peptide MALDI Imaging proved challenging. The higher laser energies needed for these MALDI experiments distorted the LCO signal. As a work-around, we collected MALDI Imaging data from consecutive tissue sections as well as performed *in situ* microanalysis of structurally annotated plaques by laser microdissection followed by immunoprecipitation (IP) based A β extraction and traditional MALDI mass spectrometry analysis (Figure 3).

Using this comprehensive microanalysis approach, we then moved on to identify plaque polymorphism associated A β signature in post mortem brain of sporadic AD (sAD) patients and CU-AP individuals. We found that the diffuse plaques in sAD and CU-AP consisted mainly of A β 1-42. A comparison of cored plaques in sAD to diffuse plaques in both sAD and CU-AP revealed that core formation in plaques was significantly associated with the deposition of A β 1-40 (Figure 4). Further, we were able to identify a N-terminal

pyroglutamate (pE) truncation of A β x-42, A β 3pE-42 and A β 11pE-42, to be the most significant difference between diffuse (and cored) plaques in AD and CU-AP where pyroglutamation was not observed.

These data suggest that non-dementia associated diffuse deposits as observed in CU-AP are chemically similar to diffuse deposits observed in sAD. However, there is an AD pathology-specific hydrophobic functionalization process of these deposits through N-terminal pyroglutamation, leading to subsequent deposition of more soluble A β 1-40 and plaque maturation into senile, cored deposits.

Most notably, these data challenge current perceptions in AD research where a) A β 3pE-42 is identified as the major component of neurotoxic plaques, and b) A β 1-42 is the major player in neurotoxic amyloid pathology.

The current data identify A β 4-42 to be the major component of amyloid plaques both in AD as well as in CU-AP, though previous data identify A β 3pE-42 as major plaque component. It appears that A β 4-42 is a major, non-disease specific metabolite of A β 1-42 that shows similar binding affinities for the A β 3pE-42 antibody, which indeed was identified by us as the major non-specific variant in all plaques.

Furthermore, although our results validate that A β 1-42 is a major component of plaques and is associated with increased pathology, it does not appear to be the major chemical signature of plaque neurotoxicity.

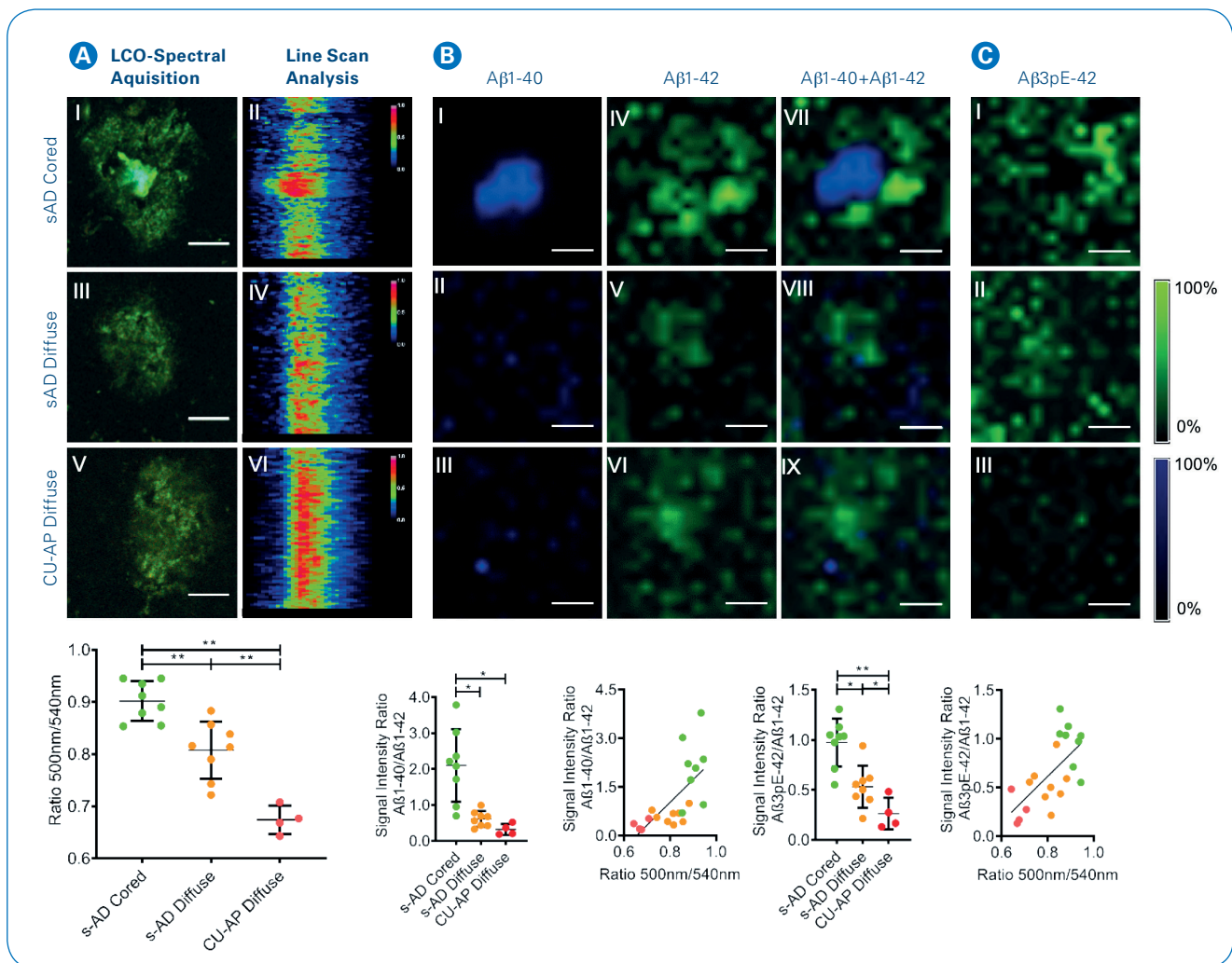


Figure 4. MALDI Imaging delineation of intraplaque A β heterogeneity. (A) LCO based hyperspectral imaging delineated plaque morphotypes, including cored- (A) (I) and diffuse- plaques in s-AD (A) (III) in comparison to diffuse plaques in CU-AP patients (A) (III). (B) (MALDI Imaging MS: Single ion images of individual plaques from MALDI IMS analysis revealed a prominent localization of A β 1-40 to the center of the cored plaques in s-AD (B) (I), while the A β 1-42 signal localized to the periphery of cored plaques in s-AD tissue (B) (IV, see also image overlay, (B) (VII). Diffuse plaques in both s-AD (B) (II, (B) (V) and CU-AP (B) (III, (B) (VI) showed low A β 1-40 signal, but a strong A β 1-42 signal, that was homogenous across these plaques as highlighted in the overlay images (B) (VIII, (B) (IX). MALDI IMS analysis did further reveal localization of A β 3pE-42 to the periphery of cored plaques in s-AD (C) (I) as well as diffuse plaques in s-AD (C) (II), while only a very low signal was present for these peptides in the diffuse plaques in CU-AP (C) (III). MALDI IMS was performed on consecutive sections to the sections used for LCO imaging and LMPC. Nr. of patients n=8 (s-AD), n=4 (CU-AP); Scale bar: (A)-(C) 20 μ m. (B)-(C) Intensity scales indicating maximum peak intensities of MALDI single ion signal.

Conclusion

- MALDI Imaging is a valuable tool to probe neurodegenerative disease pathology exceeding the capabilities of commonly used biochemical microscopy. The technique can be coupled with fluorescent chemical imaging tools to deliver orthogonal biochemical information. Application in human tissue and mouse models provide novel insights that challenge current perceptions largely deduced from limited but more commonly used biochemical staining methods.

References

- [1] Braak H, Braak E (1991). *Neuropathological staging of Alzheimer related changes*, Acta Neuropathologica, **82**, 239-259.
- [2] Murray ME, Dickson DW (2014). *Is pathological aging a successful resistance against amyloid-beta or preclinical Alzheimer's disease?* Alzheimer's research & therapy, **6**, 24.
- [3] Carlred L, Michno W, Kaya I, Sjövall P, Syvänen S, Hanrieder J (2016). *Probing Amyloid- β Pathology in transgenic Alzheimer's disease (tgArcSwe) mice using MALDI Imaging Mass Spectrometry*. Journal of neurochemistry, **138**, 469-478.
- [4] Kaya I, Brinet D, Michno W, Syvanen S, Sehlin D, Zetterberg H, Blennow K, Hanrieder J (2017b). *Delineating Amyloid Plaque Associated Neuronal Sphingolipids in Transgenic Alzheimer's Disease Mice (tgArcSwe) Using MALDI Imaging Mass Spectrometry*. ACS chemical neuroscience, **8**, 347-355.
- [5] Kaya I, Brinet D, Michno W, Baskurt M, Zetterberg H, Blennow K, Hanrieder J (2017a). *Novel Trimodal MALDI Imaging Mass Spectrometry (IMS3) at 10 μ m Reveals Spatial Lipid and Peptide Correlates Implicated in Abeta Plaque Pathology in Alzheimer's Disease*. ACS chemical neuroscience, **8**, 2778-2790.
- [6] Kaya I, Michno W, Brinet D, Iacone Y, Zanni G, Blennow K, Zetterberg H, Hanrieder J (2017c). *Histology-Compatible MALDI Mass Spectrometry Based Imaging of Neuronal Lipids for Subsequent Immunofluorescent Staining*. Analytical chemistry, **89**, 4685-4694.
- [7] Klingstedt T, Blechschmidt C, Nogalska A et al. (2013). *Luminescent conjugated oligothiophenes for sensitive fluorescent assignment of protein inclusion bodies*. ChemBiochem, **14**, 607-616.
- [8] Michno W, Kaya I, Nystrom S, Guerard L, Nilsson KPR, Hammarstrom P, Blennow K, Zetterberg H, Hanrieder J (2018). *Multimodal Chemical Imaging of Amyloid Plaque Polymorphism Reveals Abeta Aggregation Dependent Anionic Lipid Accumulations and Metabolism*. Analytical chemistry, **90**, 8130-8138.
- [9] Michno W, Nystrom S, Wehrli P et al. (2019). *Pyroglutamation of amyloid-beta₄₂ (Abeta₄₂) followed by Abeta₁₋₄₀ deposition underlies plaque polymorphism in progressing Alzheimer's disease pathology*. The Journal of biological chemistry, **294**, 6719-6732.



Learn More

You are looking for further Information?
Check out the link or scan the QR code for more details.

www.bruker.com



For Research Use Only. Not for Use in Clinical Diagnostic Procedures.

● **Bruker Daltonics GmbH & Co. KG** **Bruker Scientific LLC**

Bremen · Germany
Phone +49 (0)421-2205-0

Billerica, MA · USA
Phone +1 (978) 663-3660

ms.sales.bdal@bruker.com – www.bruker.com